STEEL FIBER REINFORCED SELF-COMPACTING CONCRETE: FROM MATERIAL TO MECHANICAL BEHAVIOR

Fatemeh Soltanzadeh, Joaquim António Oliveira de Barros and Rafael Francisco Cardoso Santos

Report: 12-DEC/E-19

This study is a part of the research project entitled "DURCOST – Innovation in reinforcing systems for sustainable prefabricated structures of higher durability and enhanced structural performance" supported by the FCT, PTDC/ECM/105700/2008.

Date: July 2012

Pages: 31

Keywords: High Performance Fiber Reinforced Concrete; Flowability; Compactness and Durability, Mechanical Characterization

School of Engineering

Department of Civil Engineering

University of Minho

Fundação para a Ciência e Tecnologia

TABLE OF CONTENTS

Page

1. INTRODUCTION

Optimization can be defined as the set of procedures used to make a system as effective as possible. Concrete is a system that has to meet varying and frequently, opposing criteria. These criteria include among others durability, strength, workability, construction operations, cost, appearance, early use requirements, rebar spacing, and availability of resources.

High and even ultra-high strength concretes were developed in recent years, with new mixture optimization techniques. That is why even the definition of 'high strength' has changed with the years. In the 80s, a compressive strength of 60 MPa would have been considered high strength; while with the term 'high strength' strengths of 80-110 MPa are associated nowadays. The compressive strength of ultra-high strength defined as 150-200 MPa and sometimes even above 200 MPa.

Increasing the concrete strength, from normal strength to high or ultrahigh strength concrete has as a consequence that the brittleness increases even more. This 'defect' can be overcome by adding fibers. Fibers increase the deformation ability and the tensile load bearing capacity of brittle materials. Without fires, high and ultra-high strength concretes can show a very sudden, almost explosive type of failure under certain loading conditions.

The employed dosage of fibers varied depending on the application (Nakamura et al. 2004). In all the aforementioned applications, one of the main advantages of using fibers is represented by the possibility of partially replacing or even completely substituting the traditional welded wire mesh reinforcement (such as shear reinforcement in beams and roof elements). This reduces the needs for manufacturing, detailing and placing the reinforcement cages and results in improved production efficiency. Furthermore, the element thickness and the structure self-weight can be also reduced, since minimum cover requirements do not hold any more (Ferrara at al. 2007).

Researches have been shown that the performance of steel fibers in the hardened-state (Grünewald, 2004; Ozyurt et al., 2007) and fresh-state (Ferrara et al. 2007) can be improved in self-compacting concrete. Through a suitably balanced performance of the fluid mixture (mainly an adequate viscosity of the fresh concrete) fibers can be orientated along the casting-flow direction. By suitably tailoring the casting process to the intended application, the direction of the fresh concrete flow, along which fibers tend to be aligned, may be made to match as close as possible to the anticipated stress pattern (i.e., the direction of principal tensile stresses) within the element when in service. This would lead to a superior mechanical and structural performance which may most likely also result into optimized structure size and reduced self-weights (Ferrara et al. 2007).

The other advantages of using SCC (especially fiber reinforced SCC) can be summarized as the good synergy between SCC and fiber reinforced technologies which improves the overall economic efficiency of the construction process; increased of construction speed, reduction of crew size and energy consumption, better working environment with reduced noise and health hazards, automation of quality control. All of the said benefits highlight the great potentials of fiber reinforced SCC in the field of sustainability (Ferrara et al, 2007). If the advantages of SCC can be combined with those inherent to HSC, the future of the consequent high-strength SCC would be promised (Grünewald and Walraven, 2009).

In the present work, the attempt is to optimize the high-strength fiber reinforced SCC mix included high shear and bending resistance which can be called as High Performance Fiber Reinforced Concrete (HPFRC). This concrete can be helpful in order to improve the bond of reinforcing bars under monotonic and cyclic loads.

The concrete is studied in two parts, named as “past” and “aggregate skeleton” parts individually. According to the concept of the present study, optimizing each of the said part can be helpful to optimize concrete entirely. Finally the optimized ratio of past and solid skeleton is discussed by the help of the experimental results.
In the paste phase, the optimized dosage of super plasticizer, fly ash and lime stone filler, are selected using the Marsh cone and Mini-slump tests. The aggregate skeleton is determined, in the second step. It is attempted to optimize the Agg. skeleton such that while the stone particles have the most compact condition in the concrete, they create the best flowability facing to the past. The final step in the mix design of the HPFRC is the choice of the paste content using the paste composition defined in the first step and the aggregate composition defined in the second step. This is achieved by determining the minimum paste volume needed for good flowability (as measured in the V-funnel and slump flow tests), low blocking and high passing ability (as measured in the L-box test), and absence of segregation. Fig.1 presents the flowchart of SCC mix designed in this study.

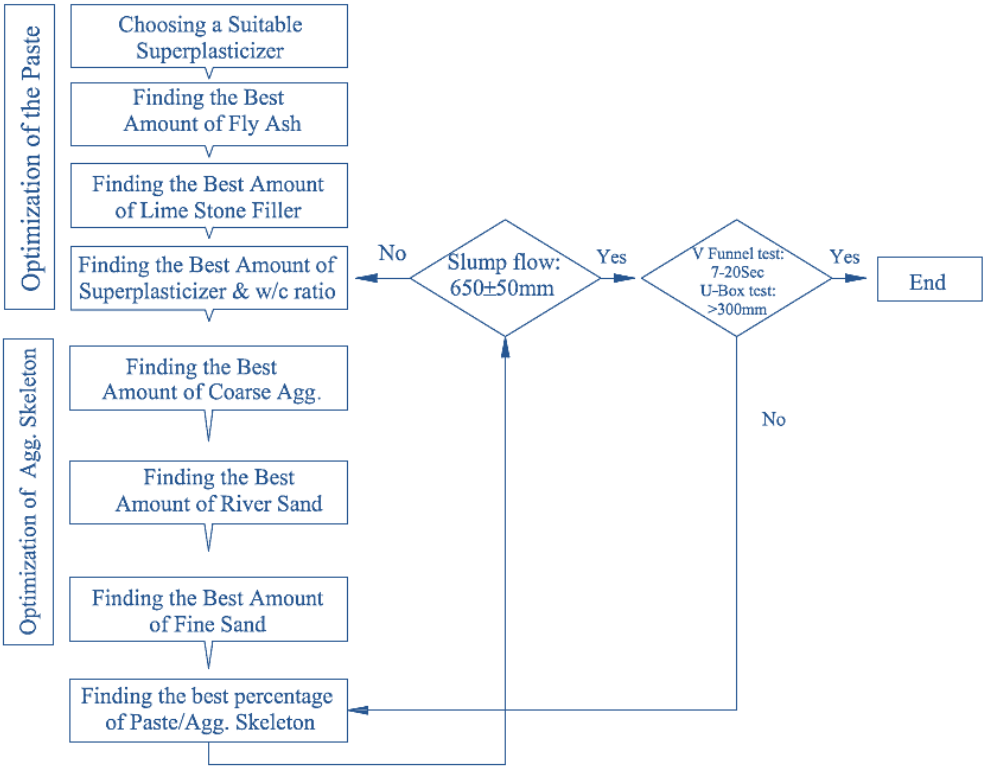

Fig.1 Flowchart of HPFRC mix design in the present study

2. REVIEW OF LITERATURE

SCC was first developed in Japan during 1986, with further mix design method introduced by professor Okamura of Tokyo university in 1993 (Choi et al, 2006). However, designing a proper SCC mixture is not a simple task. Various investigations have been carried out in order to obtain rational SCC mix-design methods. The establishment of methods for the quantitative evaluation of the degree of self-compatibility is a key issue in establishing the mix design system (Noor and Uomoto 1999). From a rheological point of view, a successful SCC is characterized by low yield stress necessary for high capacity of deformation and moderate viscosity to ensure uniform suspension of solid particles during casting (Felekoğlu et al. 2007).

Okamura and Ozawa have proposed a simple mixture proportioning system in which the coarse and fine aggregate contents are kept constant so that self-compatibility can be achieved easily by adjusting the water/cement ratio and super plasticizer dosage only (Okamura and Ouchi, 1999). Water/powder ratio is usually accepted between 0.9 and 1.0 in volume, depending on the properties of the powder (Felekoğlu et al., 2007). In order to have a very dense and compact cement matrix, generally the water cement ratio is reduced to a minimum and fine fillers, such as silica fume and fly ash, are added that fill the voids between the cement particles. Often only sand is used as the aggregate component.

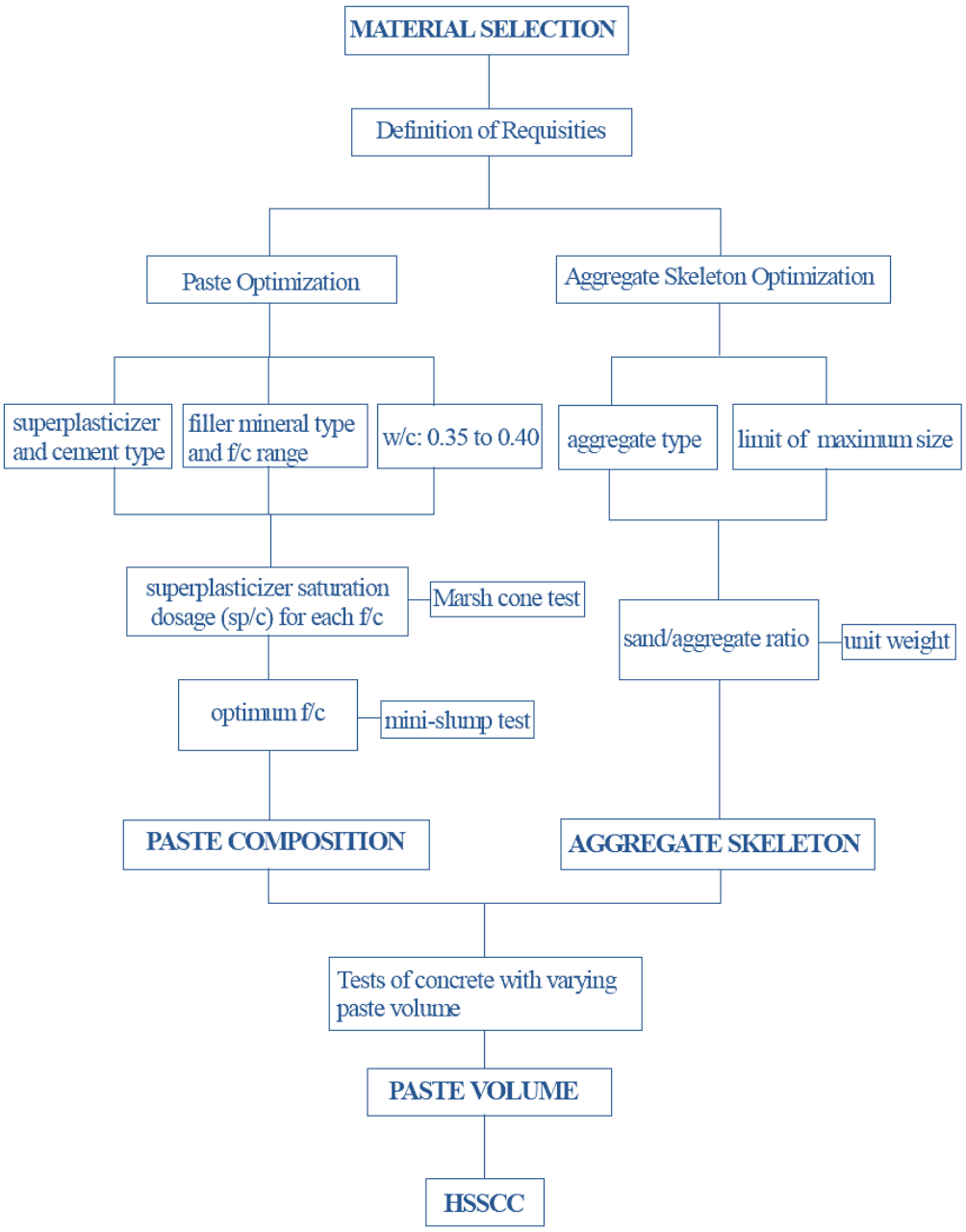

Fig.2 Flowchart of SCC mix design method, introduced by Gomes, P. C. C. (2002)

For almost 100 years, efforts have made to achieve desired concrete properties though adjustments in aggregate proportion. Initial efforts deal with the concept of maximum density with the idea that a denser gradation would contain fewer voids to be filled with

cement past. In the present study this idea will be discussed and checked experimentally. More over the results will compare with the guidelines suggested by the other researchers.

Mix method used for the self-compacting concrete is significantly different from the typical method as well as its rating standards and testing since the design of method needs to consider the two opposite properties of flowability and segregation resistance ability at the same time to assure the compacting capacity of the concrete (Choi et al. 2006). In the mix-proportioning of traditional concrete, the water/cement ratio is kept constant in order to obtain the required strength and durability. However, with SCC, the water/powder ratio has to be chosen by taking self-compatibility into account, since self-compatibility is very sensitive to this ratio (Felekoğlu et al. 2007).

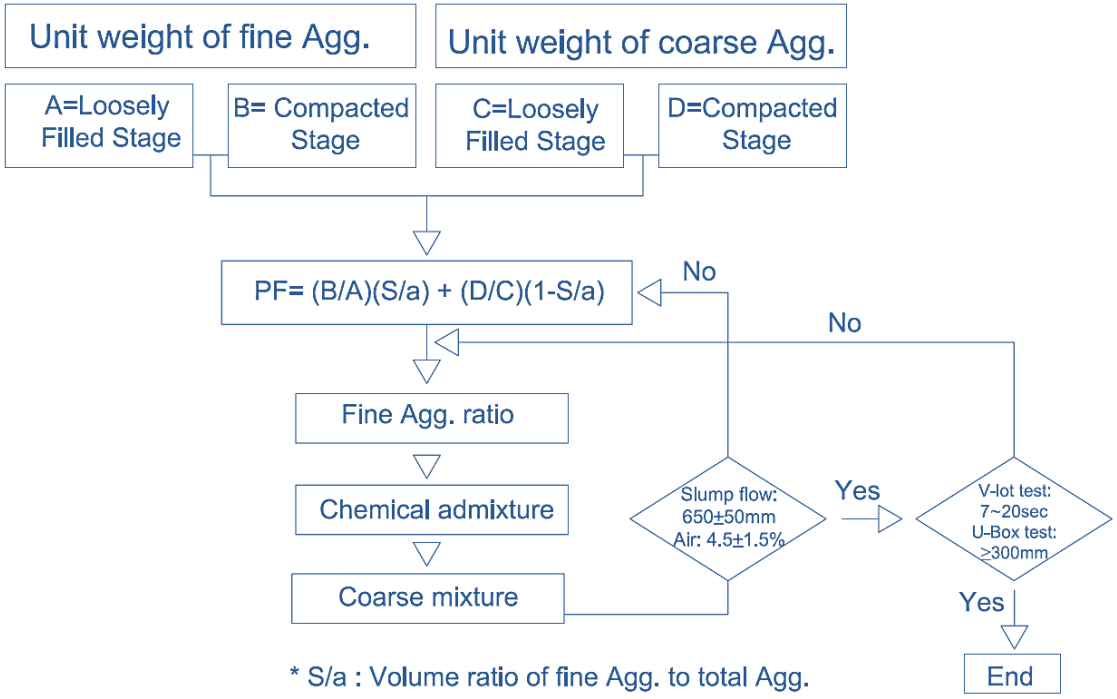

Fig. 3 Flowchart of SCC mix design method, used by Choi et al. (2006)

Gomes, P. C. C., (2002), achieved the suitable SCC mix by varying the past volume in the mix up to achieving the good fresh property. Flowchart of his mix design method is presented in Fig.2. Other researcher (Pereira, E. N. B., 2006) has used the similar method, but the percentage of w/c was not constant in his method.

Reducing the free water content (the total water minus water that is physically and chemically retained by aggregate and powder materials as well as any water bound by chemical admixtures) and increasing the concentration of fine particles can enhance the cohesion and viscosity, and hence the stability of SCC. In general, the approach of minimizing free water content to enhance stability can result in SCC mixtures with a low yield stress and moderate-to-high viscosity levels. The low water content requires a relatively high dosage of high range water reducers to obtain the required deformability especially with the lower binder contents (Felekoğlu et al. 2007). This is one of the points which are taken in to consideration in the present work.

The other method which is used to make a high strength SCC using the light weight aggregate, is the method proposed by Choi et al. (2006). Is clear in the flowchart of this SCC designed mix (Fig.2), after obtaining the PF value; the mix design process

followed by mixing the concrete with decision of fine aggregate ratio and amount of super plasticizer to review it fluidity. If in case the fluidity appears inappropriate, more proper PF values from the testing will be taken for the better mix.
Combining concrete with dispersed "fibers" consisting of grains of steel left-overs was an idea patented in 1874 by the American A. Berard (Jansson Anette, 2008). Since fibers crossing the crack guarantee a certain level of stress transfer between both faces of the crack, providing to the composite a residual strength, which magnitude depends on the fiber, matrix and fiber/matrix properties (Cunha Vitor, 2010).

3. STUDIES OF PASTE

3.1 Choosing a Suitable Super Plasticizer

Choosing a suitable super plasticizer and determining the optimum dosage of it, is fundamental to guarantee SCC properties. These admixtures permit concrete to flow, thus increasing application time and ease of use. They aid in the curing process of the concrete; prevent the concrete's components from segregating. After curing they leave the concrete with a smooth and clean surface and ensure an extremely long service life for the project.
To choose the best super plasticizer helpful enough to prepare SCC mix with a good viscosity and flowability, four different super plasticizers named as Glenium SKY 602, Glenium SKY 617, Glenium ACE 426 and Glenium 77 SCC, are studied. Table-1 presents the list of the tested super plasticizers and the allowable dosage that can be used to make a concrete mix.
Among the introduced super plasticizers, the most suitable one is chosen using Marsh cone test. Marsh cone test requires a simple apparatus that is portable (Fig. 4 a), involves the use of a small amount of material, and employs a test procedure that is easy to implement and repeat (Gomes, P. C. C., 2002). This method has been used since 1990s in concrete technology with the emergence of high performance concrete with high strength and workability, as a part of the mix design process (Gomes, P. C. C., 2002).

Table-1 Min/Max dosage of super plasticizers

Name of super plasticizer	Min/Max dosage *(Liter per 100 Kg cement)*
Glenium SKY 602	0.7/2.6
Glenium ACE 426	0.6/1.0
Glenium 77 SCC	1.3/1.9
Glenium SKY 617	0.9/1.5

Table-2 Summarized physical specification of cement type I 42.5-R

Parameter	Value
Specific gravity	3150 kg/m^3
Blaine fineness	387.3 m^2/kg
Setting time (initial)	116 min
Setting time (final)	147 min

The physical property of cement type I 42.5R which is used to make the paste is summarized as Table-2. W/c ratio is kept as 35% in order to have the good flowability without bleeding. The lower w/c ratio is not considered since the pastes flowability cannot be obtained using that ratio.

Performing the test, a certain volume of material (V) is poured into the Marsh cone. The method is based on the measurement of the time taken for a prescribed volume (v) of material to flow out of the cone. The flow time is consequently taken as an inverse of the relative measure of fluidity of the grout or paste; so that, the lower the flow time, higher is the fluidity. Based on Toralles-Carbonari et al. (1996) method, to test the flowability of the pastes are made by different super plasticizers, the cone with d = 8mm is chosen in the present study as shown in Fig. 4. The tests are performed using pastes with V = 800ml and v = 200 ml. Details of the test procedure and method of mixing are described in ASTM C939-02 and ASTM C305-91 respectively.

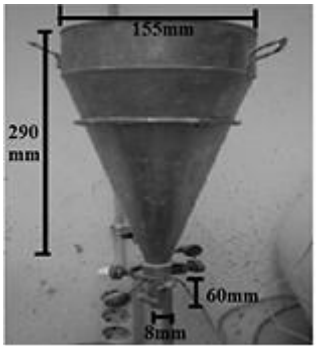

Fig.4 Marsh cone, used for optimization of super plasticizer

Table-3 Flow Time (Sec), for pastes having different sp/c

Name of Super P. \ Dosage	0.7 (%)	0.85 (%)	1 (%)	1.3 (%)	1.4 (%)	1.5 (%)	1.6 (%)	1.8 (%)	1.9 (%)	2 (%)	2.6 (%)	3 (%)	3.5 (%)	4 (%)
Glenium SKY 602	13.13		16.15		4.45		6.05	5.28		7.56	7.29	6.97		
Glenium SKY 602	13.00		16.19		5.00		5.70	5.26		7.47	7.47	6.99		
Average.	13.07		16.17		4.73		5.88	5.27		7.52	7.38	6.98		
S.D.	1.12		0.79		**0.67**		0.77	0.72		0.88	0.87	0.84		
Glenium ACE 426	13.10	8.52	8.50		7.80		7.56	9.49		7.99		8.67		
Glenium ACE 426	13.20	8.70	8.58		8.21		7.68	9.69		8.00		8.93		
Average	13.15	8.61	8.54		8.01		7.62	9.59		8.00		8.80		
S.D.	1.12	**0.94**	0.93		0.90		0.88	0.98		0.9		0.94		
Glenium 77 SCC			8.94	8.09	13.04		11.41	11.44	10.45	9.63		8.97		
Glenium 77 SCC			9.71	8.25	14.12		12.24	11.94	10.84	9.98		9.06		
Average			9.33	8.17	13.58		11.83	11.69	10.65	9.81		9.02		
S.D.			0.97	0.91	1.13		1.07	1.07	1.03	**0.99**		0.95		
Glenium SKY 617			30.01			18.31		21.2		19.36		18.34	12.9	11.87
Glenium SKY 617			38.73			19.63		22.21		20.33		18.89	12.91	12.43
Average			34.37			18.97		21.71		19.85		18.62	12.91	12.15
S.D.			1.54			**1.28**		1.34		1.30		1.27	1.11	1.08

- Cement : 1.5Kg
- w/c : 35%

The results of a series of tests performed using the same method is shown in Table-3. The mean flow time and standard deviation (S.D.) for each paste are determined in the case of each super plasticizer. It is clear that the flow time generally decreases with increasing the dosage of super plasticizer (sp/c). Beyond a certain dosage the flow time does not decrease significantly. This particular dosage is defined as the saturation or optimum dosage. Type of cement and super plasticizer, type and dosage of mineral admixture, w/c ratio and mixing sequence can affect the saturation dosage. In general, the saturation dosage leads to high fluidity in the paste without causing bleeding or segregation (Gomes, P. C. C., 2002).

The determination of the saturation dosage can be according to the shape of the curve. According to the different researchers, the saturation point can be determined as:

1) The lowest sp/c ratio for a tangent in the plot of the logarithm of flow times versus sp/c ratio with a slope of 2/5, (presented in Fig.2 (a)) (De Larrard et al., 1997); or
2) The dosage where the flow time versus sp/c ratio curves at 5 and 60 minutes intersect, (presented in Fig.2 (b)) (Aïtcin, 1998); or
3) The logarithm of the flow time versus sp/c ratio (in %) should be plotted, as shown in Fig. 2 (c); and the internal angle α should be determined at each data point. The saturation point is taken as the dosage where α is within interval $140^{o}\pm10^{o}$ (Gomes, P. C. C., 2002).

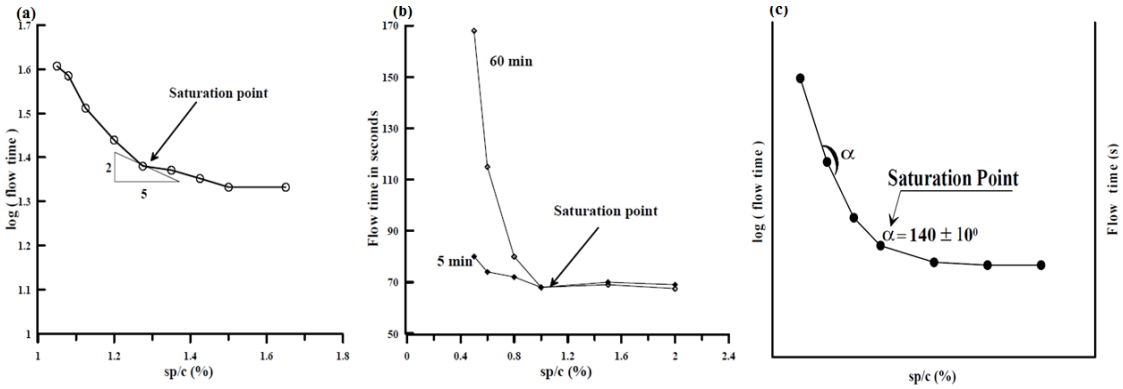

Fig.2 Procedures for the determination of the saturation point: (a) Method of De Larrard (b) Method of Aïtcin., (c) Method of Gomes (Gomes, P. C. C., 2002)

In the present study, the third method is chosen to find out the saturation point. It is tried to choose the same percentage of super plasticizer to the paste in each series in order to have the possibility of comparing the effect of the different super plasticizers. As it is mentioned in Table-1, the minimum and maximum dosages of the super plasticizers are different which makes a small difference in the selection of dosages. Fig. 3 (a) shows the decrease of Marsh flow time by increasing the percentage of super plasticizer up to the optimum point or saturation point. After the saturation point, flow time shows the constant trend or very marginally decreasing/increasing trend. It is visible that the past contains Glenium SKY 602 super plasticizer, shows the better workability as compare to the pastes contain the other types of super plasticizer. The series of paste contains Glenium ACE 426, Glenium 77 SCC, and Glenium SKY 617 respectively shows the lower workability. By determining the internal angle at each point of the graph "Logarithm of flow time vs. the percentage of super plasticizer," (shown in Fig. 3), the saturation point in each curve is detected. The saturation point is marked with unfilled point in each curve. Among the tested pastes, the one contains Glenium SKY 602 is shown the highest flow time and highest viscosity at the saturation point. So that, Glenium SKY 602 is consider as the suitable super plasticizer for making the concrete mix. Glenium SKY 617 shows the list flow time and might be effective to have the good viscosity in the pastes. Thus Glenium SKY 602 and Glenium SKY 617 are the two super plasticizers which are used for optimizing the percentage of fly ash as discussed in the next section.

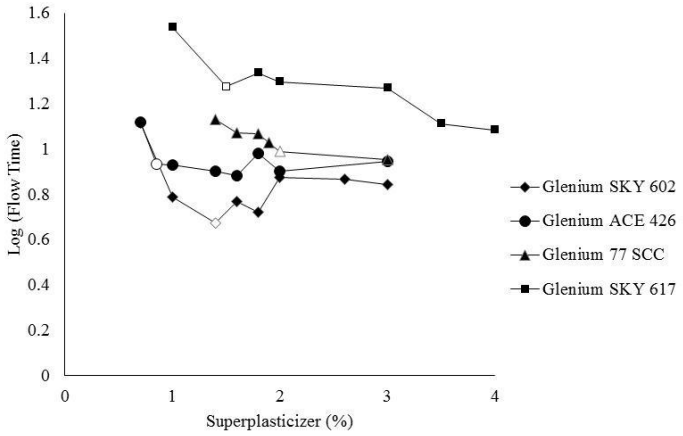

Fig.3 Marsh flow time vs. the percentage of super plasticizer

3.2 Optimization of the Fly Ash

Cement is one of the most expensive components of concrete. Although cement paste is required to fill aggregate voids, bind them together and provide mobility to fresh concrete, it is also responsible for drying shrinkage, heat generation and porosity. Consequently, minimizing the amount of cement paste would be one of the goals of concrete optimization. Fly ash is generally used in concrete at replacement levels of up to 30 %, and it should comply with EN 450 and ASTM C 618. It improves fluid behavior of concrete mixes, due to the spherical shape of their constituting particles. These microscopic spherical particles act as micro-rollers, decreasing friction and flow resistance, and improving packing density (Pereire E. 2006).

Although fly ash is a very inhomogeneous material, class F fly ash enhances cement hydration at a larger extent; increase the dense of microstructure and concrete strength and durability. This is related with two distinct mechanisms:

1) Fly ash particles occupy the empty spaces between cement particles; due to their smaller size, they act as nucleation points and improve space for a better growth of the hydration products;

2) Fly ash is able to react with Ca2+ and OH- ions released by the cement to form secondary products. Consequently, it may be considered as a pozzolanic material (Chandra, 2002).

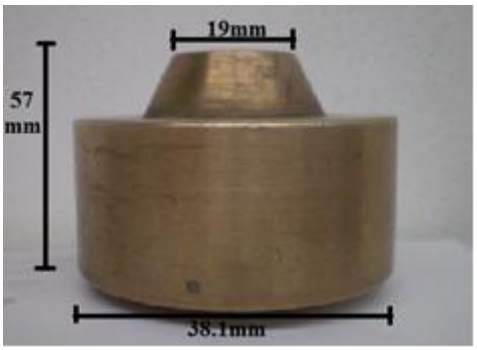

Fig. 4 Mini slump, used for optimization of the past

To detect the optimum percentage of fly ash which its properties is reported in Tbale-4, two series of flow tests is carried out for the paste included the minimum percentage of one of the selected super plasticizers, Glenium SKY 602 and Glenium SKY 617. The tests are performed using the mini slump as shown in Fig. 4. In addition to the said

super plasticizers, the paste includes fly ash, cement and water. The ratio of w/c is chosen 28% considering having the proper workability and no bleeding in the past. To increase the flowability of the paste, different percentage of fly ash (Fig.5) is replaced by the cement volume. The procedure of mixing the material is as addressed in section 1.3.

Table-4 Physical property of fly ash (Pereira, E. 2006)

Parameter	Value
Specific gravity	2360 kg/m^3
Blaine fineness	387.9 m^2/kg
Particles < 75mm	81.15-94.40 %
Particles < 45mm	68.45-85.90 %

Results of the test presented in Fig.5, show the improving trend of flowability of the past by replacing of the fly ash with that of cement. This increase is more sharply by addition of up to 25% fly ash. The effects of fly ash decreased from the same point such that the relative spread of the past is shown marginal difference in the case of the pastes include 35% to 55% fly ash. Comparing the curves in Fig.5, it is clear that the flowability of the pasts contain 35% to 55% fly ash, is almost the same. This point shows the similar effect of two different super plasticizers on the past. This effect is not the same before the addition of 35% fly ash. It should be taken in to consideration that the relative spread of the past contained Glenium SKY 617 is always higher than that of the paste made by Glenium SKY 602.

It was observed that a film of water is appeared on the surface of the paste contain 25% or higher percentages of fly ash and Glenium SKY 602. The same phenomenon is observed for the past made by Glenium SKY 617 after addition of 40% fly ash (Fig.6). Since the bleeding is happened later in the past contains Glenium SKY 617, it is decided to continue the study of the past using Glenium SKY 617 only in order to control the bleeding easier. Moreover, from the curve it can conclude that 35% is the maximum amount of fly ash after which the relative spread of the past approximately follows the constant trend. This point is shown as the unfilled points in Fig.5.

The new series of test is carried out to find out the optimum percentage of fly ash, when the percentage volume of fly ash does not replace by the cement volume but added to that of cement. The ratio of w/c is chosen as 0.24 and the minimum dosage of Glenium SKY 605 is used for making the past. Similar to the previous series of tests the increase in flowability is observed by increasing the percentage of fly ash (Fig.7).

The addition of 30% fly ash cased the maximum spread in the past. Higher percentage of fly ash decreases the flowability of the past very marginally. Addition of fly ash up to 35% does not case bleeding; while after addition the higher percentages, the slim film of water is observed on the surface of the spread paste.

The new series of test is followed thereafter using Glenium SKY 617 super plasticizer only. This time, the paste is made by addition of different dosage of fly ash to the cement and not replacing with cement. The visual changes in the flowability of the past up to occurrence of the bleeding are shown in Fig.8. The average diameter of the past measured during flow test is noted as Table-5.The bleeding of the paste which is started by adding more than 35% fly ash is visible in Fig.8. The location of bleeding is marked in images No. (5) of Fig. 8.

Similar to the previous tests, it is found that the maximum relative spread of the paste is occurred by addition of 30 or 35% fly ash to the mix. Tacking in to consideration the results of the tests illustrated in Figures 5 and 7, it is decided to continue the study using

the pasts contains 30% or 35% fly ash as the optimized percentage of fly ash. The best percentage of fly ash is decided in the next stage.

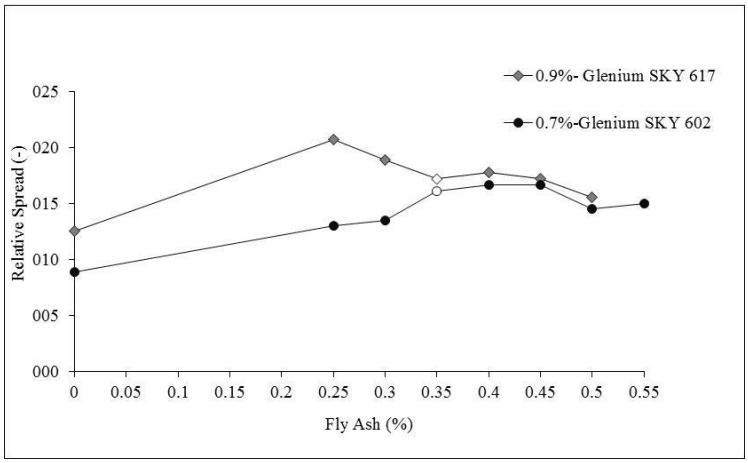

Fig.5 Relative spread of paste made by two different super plasticizers

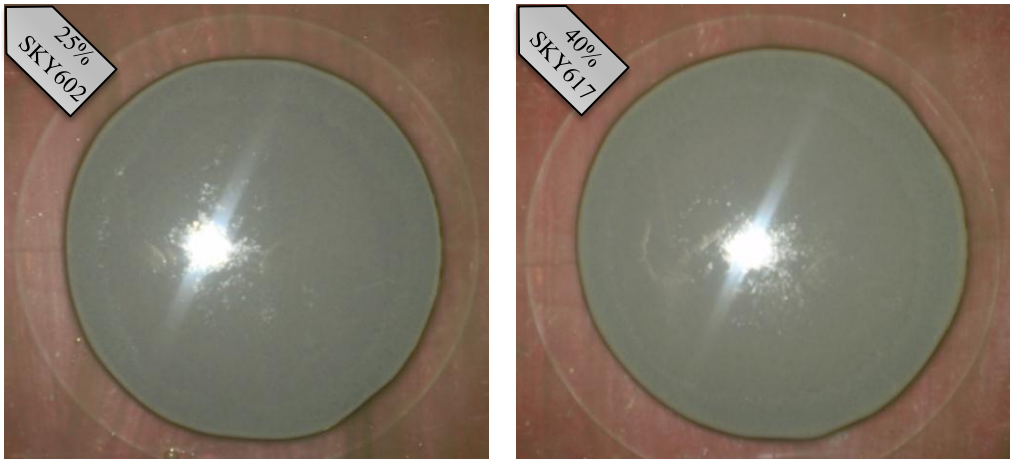

Fig.6 Bleeding of the past (right) made by Glenium SKY 602 after addition of 25% fly ash, (left) made by Glenium SKY 617 after addition of 40% fly ash

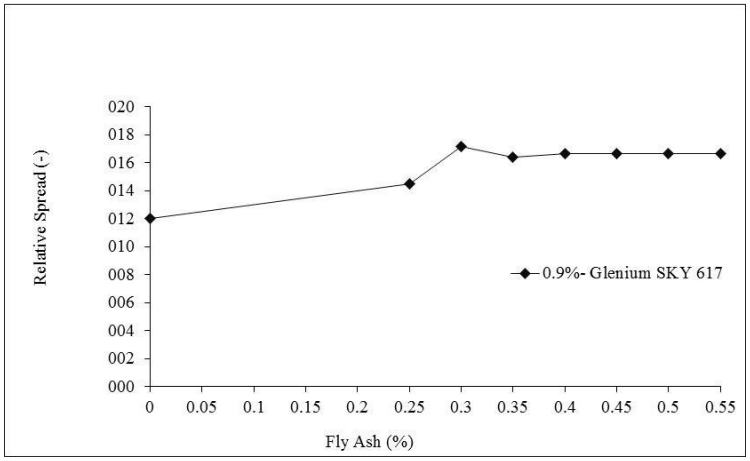

Fig.7 Relative spread of paste after addition of different percentage of fly ash to cement

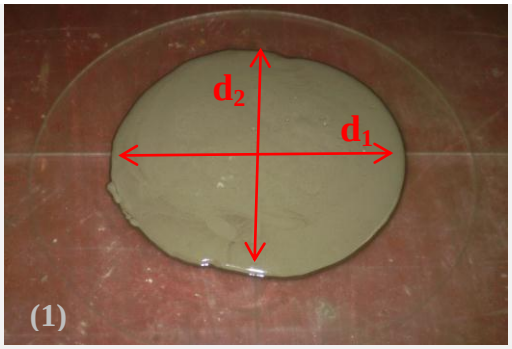

- 0.7% Glenium SKY 617,
- Without Fly Ash,
- Low flowability and not sufficient spread of the past.

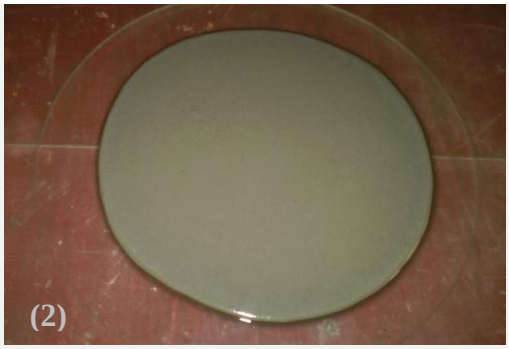

- 0.7% Glenium SKY 617,
- 25% Fly Ash,
- Better flowability and observing the smooth paste without bleeding.

- 0.7% Glenium SKY 617,
- 30% Fly Ash,
- Improving the flowability without bleeding.

- 0.7% Glenium SKY 617,
- 35% Fly Ash,
- Improving the flowability with an ignorable bleeding.

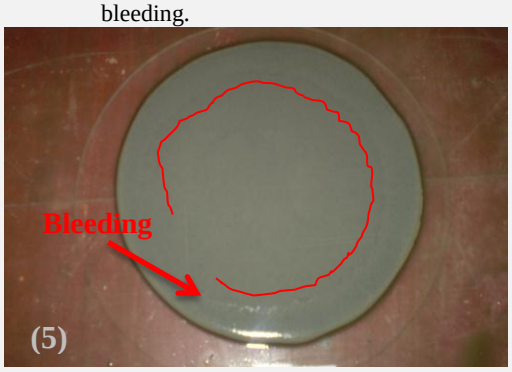

- 0.7% Glenium SKY 617,
- 40% Fly Ash,
- Almost no change in the flowability and observing the bleeding.

- 0.7% Glenium SKY 617,
- 45% Fly Ash,
- Same flowability and bleeding.

- 0.7% Glenium SKY 617
- 50% Fly Ash
- Same flowability and increasing of bleeding.

- 0.7% Glenium SKY 617
- 55% Fly Ash
- Same flowability and bleeding.

Fig.8 Flowability of the paste made by different dosage of fly ash

Table-5 Diameter of the past contains different dosage of fly ash

Dosage of fly ash *(%)*	Diameter of the paste		Average *(mm)*
	(d_1)(mm)	*(d_2)(mm)*	
0	13.5	14	13.75
0.25	15.00	15.00	15
0.3	16.00	16.50	16.25
0.35	15.80	16.00	15.9
0.4	16.00	16.00	16
0.45	16.00	16.00	16
0.5	16.00	16.00	16
0.55	16.00	16.00	16

- w/c : 0.24
- Super plasticizer : 0.9% Glenium SKY 617

3.3 Optimization of Lime Stone Filler

Limestone powders produce the more compact structure by pore filling effect. Farther more it is helpful to develop the paste composition, filling the voids between the cement particles, increasing the dense, strength and durability properties of concrete (Ravikumar, et al. 2009). In the previous section the optimum percentage of fly ash is chosen. To determine the optimum percentage of lime stone filler which should be added to the past, the same type of tests were performed on paste compositions with cement, super plasticizer (0.9% of cement weight), fly ash (30% and 35% of cement weight), w/c ratio of 0.23 and different percentages of lime stone filler. The results obtained for relative spread of the pasts are represented in Fig.9. It is clear that, with increase the amount of limestone filler, the relative spread increases almost linearly up to addition of 30% lime stone filler. Beyond this point, the change in the flowability of the past is very marginal. Comparing the carves of the same figure shows that the pasts contain up to 30% of lime stone made with 30% fly ash are more flow able than that of contain 35% of fly ash. The past contains 30 and 35 percent fly ash are shown the same flowability by adding 35% lime stone filler to the past. By adding more that 35% lime stone filler, the flowability of the past included 35% fly ash is marginally higher than that of the past with 30% fly ash.

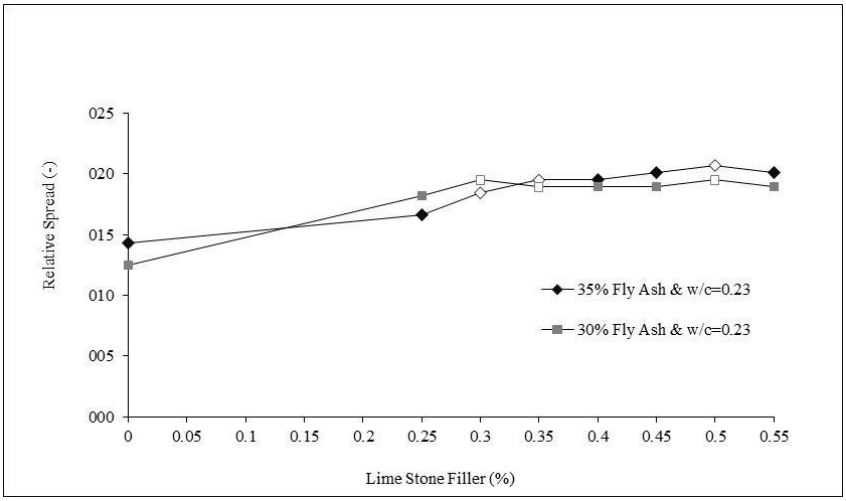

Fig.9 Relative spread of paste after addition of different percentage of lime stone filler

- 30% Fly Ash,
- Without Lime stone filler,
- good flowability and no bleeding.

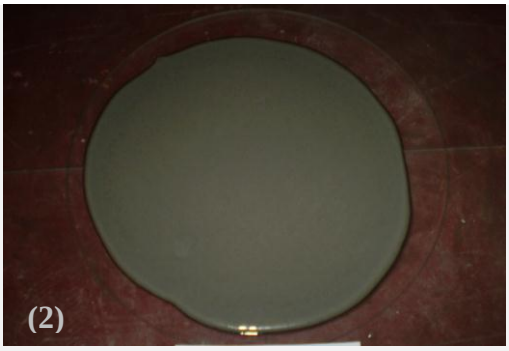

- 30% Fly Ash,
- 25% Lime stone filler,
- Improving flowability and no bleeding.

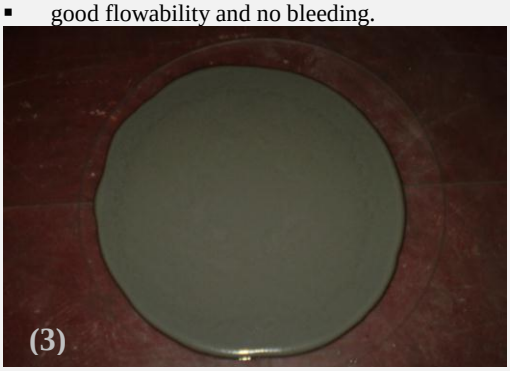

- 30% Fly Ash,
- 30% Lime stone filler,
- Improving the flowability and observation of the negligible film of water on the surface.

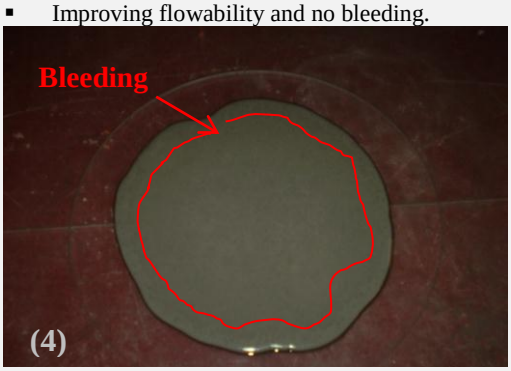

- 30% Fly Ash,
- 35% Lime stone filler,
- Same flowability and observation of the bleeding.

- 30% Fly Ash,
- 40% Lime stone filler,
- Same flowability and bleeding.

- 30% Fly Ash,
- 45% Lime stone filler,
- Same flowability and bleeding.

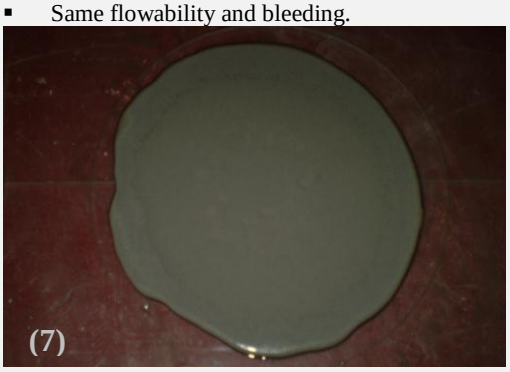

- 30% Fly Ash,
- 50% Lime stone filler,
- Same flowability and bleeding.

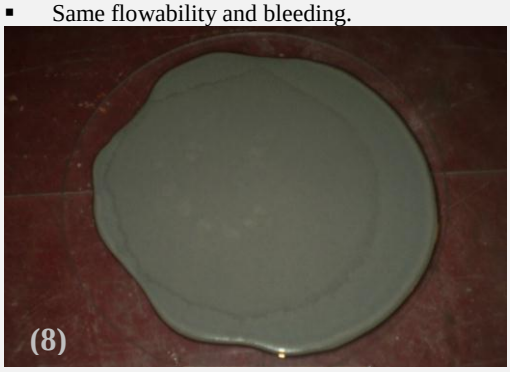

- 30% Fly Ash,
- 55% Lime stone filler,
- Marginal Improving of flowability observing the bleeding.

Fig.10 The paste made by 30% fly ash and different dosages of Lime stone filler

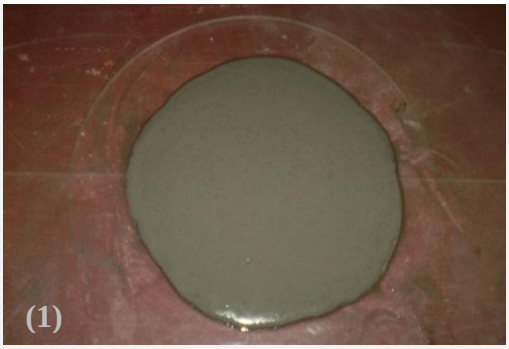

- 35% Fly Ash,
- Without lime stone filler,
- Good flowability and no bleeding.

- 35% Fly Ash,
- 25% Lime stone filler,
- Improving the flowability and observing a negligible file.

- 35% Fly Ash,
- 30% lime stone filler,
- Marginal improve of the flowability and observing a negligible film of water on the surface of the paste.

- 35% Fly Ash,
- 35% lime stone filler,
- No change in flowability and observation of the same negligible bleeding.

- 35% Fly Ash,
- 40% lime stone filler,
- Marginal increase of flowability and bleeding.

- 35% Fly Ash,
- 45% lime stone filler,
- Same flowability and bleeding.

- 35% Fly Ash,
- 50% lime stone filler,
- Same flowability and bleeding.

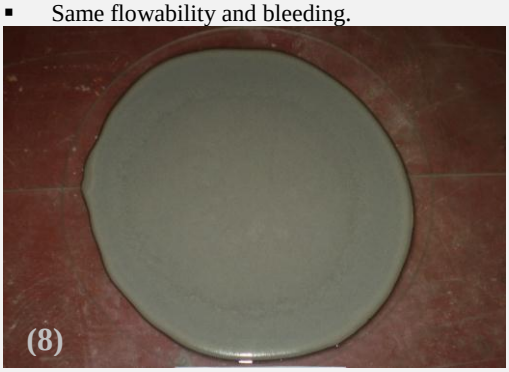

- 35% Fly Ash,
- 55% lime stone filler,
- Same flowability and bleeding.

Fig.11 The paste made by 35% fly ash and different dosages of Lime stone filler

During performing the test no bleeding is observed in the case of both groups of pasts (contain 30% and 35% fly ash), up to the addition of 30% lime stone filler. A film of water is appeared on the surface of the spread past by adding the higher percentage of lime stone filler as shown in Fig. 10 and 11respectively.
The suitable percentage of lime stone filler which is chosen to test the compressive strength of the past is marked as the unfilled points in Fig.9. Since the flowability of the past made by 30% to 50% lime stone filler is almost the same, it is decided to test the compressive strength of the mortar made by these series of pasts to choose the best percentage of lime stone filler. Compressive strength tests are performed according to ASTM C39 / C39M – 05. As it is shown in Fig.12, the compressive strength of $50 \times 50 \times 50 mm^3$ specimens decreased by increasing the percentage of lime stone filler.
The specimens included 30% flay ash is shown a bit higher strength as compared to that of specimens included 35% fly ash, due to the pozzolanic effect of fly ash. Adding beyond 30% lime stone filler, the compressive strength of the pastes included 30% and 35% fly ash is shown almost the same compressive strength.
A film of water is observed on the surface of the past by adding more than 30% of lime stone filler. To prevent the bleeding phenomenon and having the same compressive strength using the understudy past, it is decided to choose the past includes 30% fly ash and 30% lime stone filler.

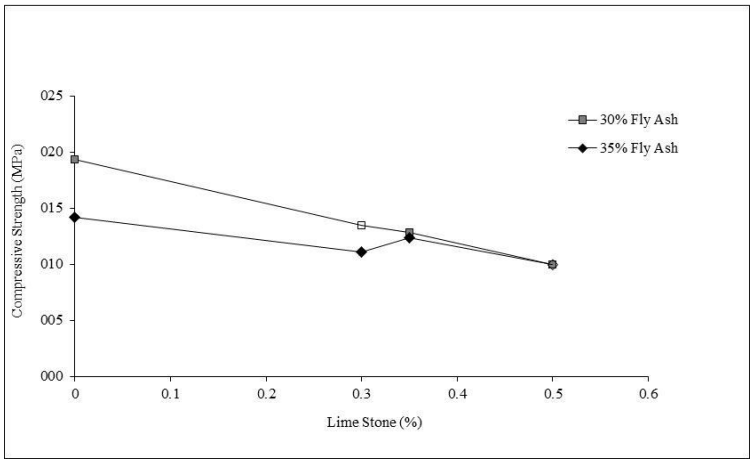

Fig.12 Compressive strength of different percentages of lime stone filler

3.4 Optimization of Super Plasticizer

By having the optimized dosage of fly ash and lime stone filler, the tests are carried out to determine the optimum dosage of Glenium SKY 617 super plasticizer. Thus some past composition with distinct percentage of super plasticizer is produced, keeping constant all the other components. The w/c ratio is kept 0.26. The amount of super plasticizer is varied between 0.7 to 2.6%, defined in terms of volume relatively to the fine materials total volume. For each sample, the relative spread, the flow time using Marsh cone and the dosage of super plasticizer at the saturation point is measured. The obtained results are indicated in Fig.13.
According to Fig.13 (right), 1.2% super plasticizer can be the saturation dosage. However the marginal bleeding is observed on the surface of the paste cause to accept the 1% super plasticizer as the optimum dosage. In the next stages it is tried to apply super plasticizer higher than 1% to obtain the exact optimum value of it.

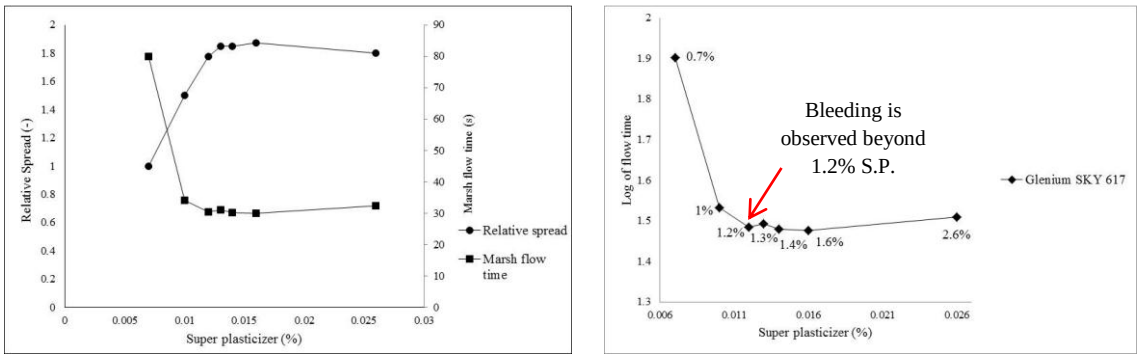

Fig.13 (left) Flow time and relative spread of paste after addition of different percentage of super plasticizer and (right) marsh flow time vs. the percentage of super plasticizer

4. STUDIES OF AGGREGATE SKELETON

In order to design a HPFRC, the size and quantity of the aggregates have to be carefully selected in such a way that a very dense and compact skeleton can be made. If aggregate voids are minimized, the amount of paste required for filling these voids is also minimized maintaining workability and strength. However, making such composition should be made such that the workability of the concrete does not decrease. Consequently, optimal mixture proportioning will produce good-quality concrete with a minimum amount of cement. Within limits, the less paste at a constant water-cement ratio, the more durable the concrete (Shilstone, 1994).

Research shows that there is a clear relationship between shape, texture, and grading of aggregates and the voids content of aggregates (Dewar, 1999). In fact, flaky, elongated, angular, and unfavorably graded particles lead to higher voids content than cubical, rounded, and, well-graded particles.

In the present study, three types of aggregates: Coarse Aggregate, River sand and Fine Sand which is shown in Fig.13 (a) from left to right respectively, are included in the aggregate skeleton of the concrete. The sieve analysis and the property of these aggregates are presented in Fig. 14 and Table-6 respectively. Comparing the shape of coarse aggregate which is chosen in the present study, with that of the charts provides by Ahn (2000) (Fig.13 (b)) for the visual assessment of particle shape, the coarse aggregate can be called as angular aggregates. Angular particles tend to increase strengths (Kaplan 1959). However there are more voids between these particles and require more sand to fill voids and to provide workable concrete (Legg, 1998). Thus, it is tried to fill the voids created between the crushed aggregate using well-graded river sand and fine sand. The coarse aggregate used as the stone skeleton has the rough surface. This aggregate can be helpful in order to increase the compressive and flexural strength of concrete (Quiroga P., et al. 2004).

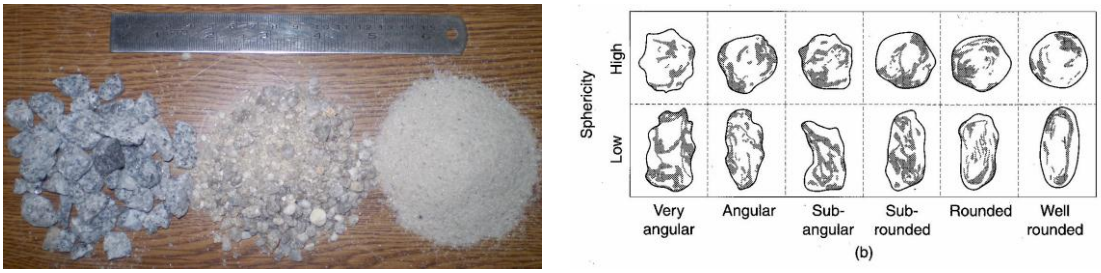

Fig.13 (a) Aggregates used in the present study **(b)** Visual assessment of particle shape based upon morphological observations (Quiroga P., et al. 2004)

The shape and texture have a direct effect on strength by influencing stress concentrations in the composite material; the degree of micro-cracking and crack branching before and during failure; and macro and micro-roughness effects at interfaces (Alexander, 1989). The shape and texture affect the shape of the stress-strain curve of concrete as they influence micro-cracking in the transition zone (Mehta and Monteiro 1993).
The effects of shape and texture of fine aggregate are much more important than that of coarse aggregate (Quiroga P., et al. 2004). The sand used in the present study, is approximately spherical particles requires less paste and less water for workability than the other shapes of aggregates. It also leads to better pump ability and finish ability as well as produce higher strengths and lower shrinkage than flaky and elongated aggregates (Shilstone, 1990).

Table-6 Aggregate properties

Aggregate	Specific Gravity *(kg/m^3)*	Absorption *(%)*	Maximum size *(mm)*
Fine Sand	2.609	10.64	12.5
River Sand	2.630	5.08	4.75
Coarse Aggregate	2.613	1.58	2.36

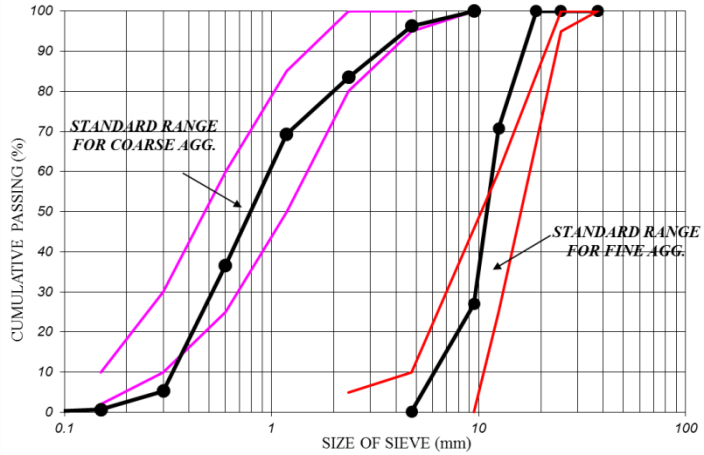

Fig.14 Sieve analysis of the used aggregates

In the present study, the optimum dosage of three kinds of aggregates: Coarse Aggregate, River sand and Fine Sand included in the Agg. skeleton of the concrete is determined based on the better compaction of the aggregates. According to shilstone J.M. and J.M. Shilstone Jr. (1987) recommendation, the aggregate gradations are determined on the basis of volume rather than the traditional weight. This makes more sense because particles interact volumetrically and not by weight.
In accordance with ASTM C 29, the shoveling procedure was the adopted one to access the bulk density of the mix of the three types of aggregates. Like so, the bulk density of each mix was measured for aggregates in a loose condition. This method is used by the idea that during mixing and placing operations of self-compacting concrete mixes, the aggregates behave closer to the loose condition than to the compacted one. Since the fibers should be placed between the stone particles, the volume of the measurement cone which is used for this test is equal to the summation of coarse aggregate, fine sand

and river volumes only. Two different methods were used to find out the best composition as follow:

4.1 Determination of the Optimum Dosage of Solid Skeleton: Method No. 1

By using this method to determine the optimum dosage of the solid skeleton, the test is carried on based on an indirect assessment of packing density by measuring the weight of each mix. Initially, only coarse aggregate and fine sand are used for testing. 2.5cm^3 coarse aggregate is chosen to fill the measurement con with the same volume. To place the aggregates properly, the cylinder contains the aggregate is vibrated 2 times for 3 seconds. Similarly some compositions of coarse aggregate and river sand in different proportions with 2.5cm^3 total volume is then made, and the total weight of the aggregates placed in cylinder is measured. In addition to the aggregates, 90kg/m^3 fibers which its property is introduced as Table-7 is included to the cylinder.

The obtained results are clearly shown in Fig.15. The maximum point in this curve corresponds to the 'heaviest mix', or in the other words, to the most compact one which is marked as the unfilled point. These compositions are respectively introduced as S1, S2 and S3 in Fig. 15. The optimum percentage of river sand can be added to the coarse aggregate to have the maximum weight is 70% of that of the coarse aggregate.

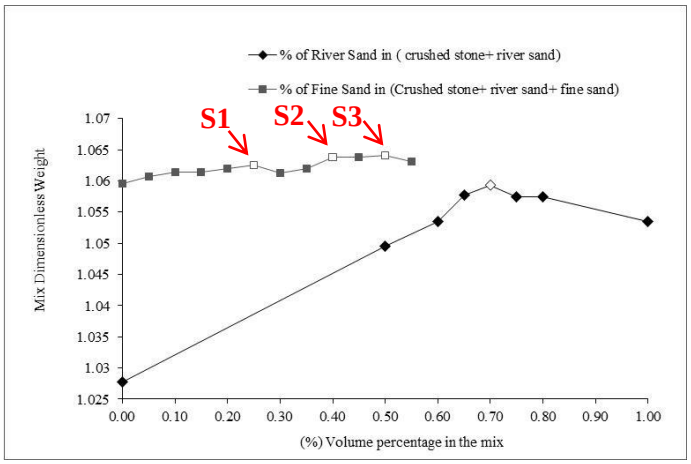

Fig.15 Determination of the optimum composition of the solid skeleton

Table-7 the fiber property used in the present research

Fiber qualification	Performance Characteristics
Diameter	0.85 mm
Length	30 mm
Aspect ratio	35
Tensile strength	1100 MPa
Profile	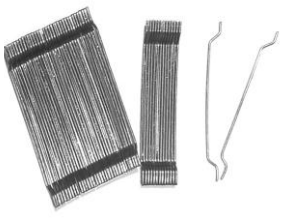

In order to increase the compaction of the solid skeleton and find the optimum percentage of fine sand, another series of mixes are made. The relative percentage of river sand and crushed stone determined in the forward stage is kept 70% constant,

while the percentage, in volume of the fine sand is varied. The best volume percentage of fine aggregate in the said composition (25%, 40% and 50%) is marked as unfilled point in Fig.15. Performing these tests leads to detect 3 different compositions of stone contains the percentage of coarse aggregate and river sand and different percentages of fine sand.
Calculation of aggregate volume in this series of tests is such that by adding sand, continuously the volume of coarse aggregate is reduced while the volume of sand is increased. On the other words the sand particles is replaced by the percentage of coarse aggregate while it is placed in the voids which are created between the coarse aggregates. Thus, placing the solid particles in the cone is easier by increasing the amount of fine aggregates. However in last stage of this test, it is observed that the solid composition cannot fill the con properly although the volume of all the prepared compositions is kept constant. Additionally, decreasing the size of solid particles due to replacing the finer aggregate with the coarser one; the compressive strength of concrete decreases. As coarser the solid particles are in the composition, the higher is the concrete strength.
Due to the said reasons the second series of test is performed in which the sand is added to the constant volume of coarse aggregate in order to fill the voids between the coarse aggregates in each stage. Since the lower the content of sand the more pronounced is the negative effect of fibers on the packing density (Grünewald and Walraven, 2009), it is attempted to add the maximum percentage of sand.

4.2 Determination of the Optimum Dosage of Solid Skeleton: Method No. 2

This series of test is performed in order to fill the voids created between the coarse aggregate of solid skeleton more effectively than the previous method. To find out how much is the empty space between the coarse aggregates, initially the wet cylinder with 2.5cm^3 volume is filled up by the saturated coarse aggregate and wet steel fibers. The cylinder has poured with water then. The measured volume of water placed between the coarse aggregates is almost equal to the volume of voids. Knowing the volume of empty voids is helpful to detect the percentage of empty space which should be filled by sand.

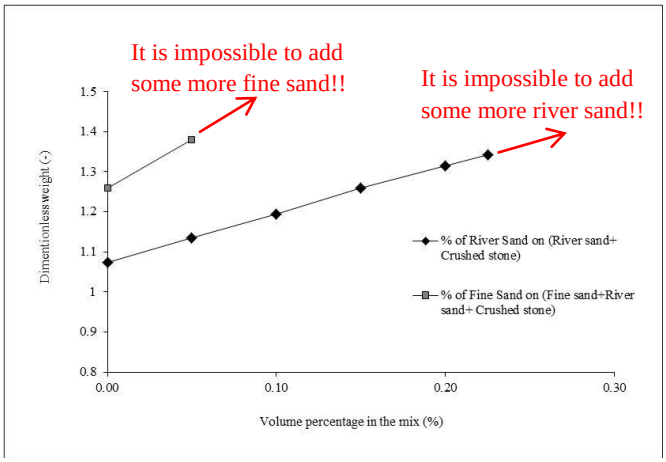

Fig.16 Determination of the optimum composition of the solid skeleton

In the next step, the volume of coarse aggregates is kept constant, equal to the volume of the cylinder and the river sand is added gradually. By adding river sand the voids are filled and the weight of the composition increased up to the time that there is no void to fill with river sand. Thereafter the fine sand is added to fill some smaller voids which

lead to increase the weight of the composition. The trend of optimization of the solid skeleton in using the second method is illustrated in Fig.16.
Although it is impossible to add more sand at the end of the test, the volume of sand which fills the voids is less than that of water. It is assumed that this empty spaces will be filled by past. Fig.17 shows differences between this method and the previous one. During the test it is detected that the volume of coarse aggregate used to fill the voids in the second method of making the solid composition is 24.77% higher than that of measured in the first method. The amount of river sand and fine sand are calculated respectively 16.8% and 7.98% lower in the second method of testing as compare to that of the first series. Table-8 shows the dosage of solid particles calculated using two methods of testing.

Table-8 Percentage of coarse Agg., fine and river sand in different compositions

Composition name		Coarse Agg. *(%)*	River sand *(%)*	Fine Sand *(%)*	Total Weight *(gr)*
Method No. 1	S.1	51.28	35.90	12.82	3786.09
	S.2	47.62	33.33	19.05	3788.77
	S.3	45.45	31.82	22.73	3790.36
Method No. 2	S.4	76.05	19.10	4.84	3968.2

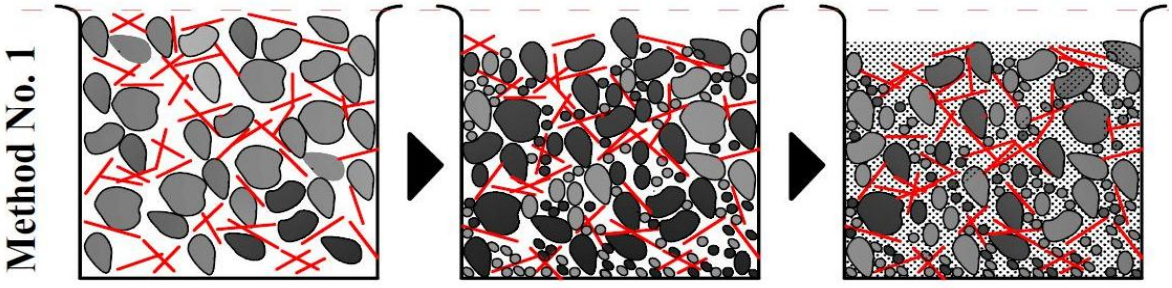

(1) Filling the cone with coarse Agg. And fibers,	(2) Replacing a percentage of river sand, with coarse Agg., and	(3) Replacing a percentage of fine sand with the composition of coarse Agg. +river sand.

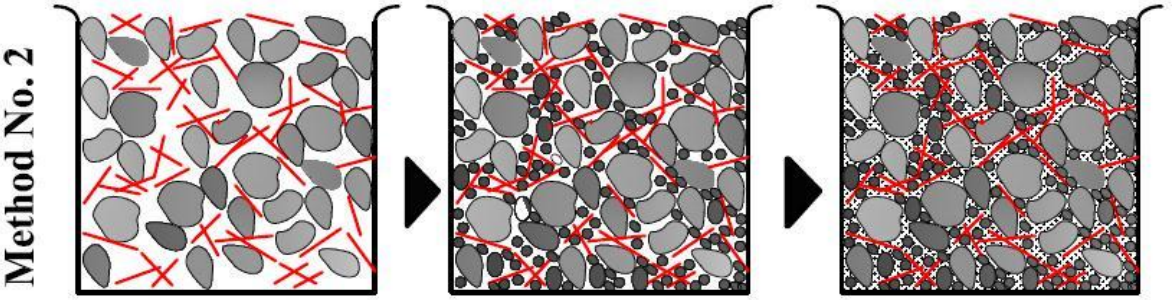

(1) Filling the cone with coarse Agg. And fibers,	(2) Addition of a percentage of river sand to the coarse Agg., and	(3) Addition of a percentage of fine sand to the composition of coarse Agg. + river sand.

Fig.17 Procedure of the optimization of stone skeleton using methods No. 1 and 2

The different methods to predict the effect of stone skeleton on the workability of concrete have been developed in many researches and guidelines (Minnesota DOT,

Shilstone (1970's), UASF (1997), and ASTM C33, etc.). Must of this methods are like the gradation portrayal of an individual percent retained verses sieve size chart.
According to ACI 302.1R-96, to obtain a desirable matrix and reduce water requirement, a uniform gradation is important. It notes that to reduce water demand while producing good workability, the severe gape-grading or excessively coarse or fine grading should be prevented. The minimum and maximum limits for the individual percent of aggregates which should retain on different sieve sizes are recommended by Minnesota DOT as a graph. The results achieved from this part of study is plotted in Fig.18 (for composition S.1, S.2, S.3 and S.4) and compared with Minnesota DOT graph.
Comparing the results achieved from the first method of testing related to the S.1, S.2 and S.3 compositions (Fig.18), shows that increasing the percentage of fine sand in the composition leads to have the less percentage of large stones; the composition has the higher weight and thus includes less voids. Composition "S3" which is plotted by the help of the results achieved using the second method of testing, shows that the composition includes the high percentage of large stones; so that there is a gap between the amount of coarse and sand aggregates in the composition. However this composition is the heaviest composition achieved in this part of study. It means that this stone composition may be very helpful to get the good compressive strength in the case of normal concrete but it may not be helpful to have the high workability in the case of SCC.

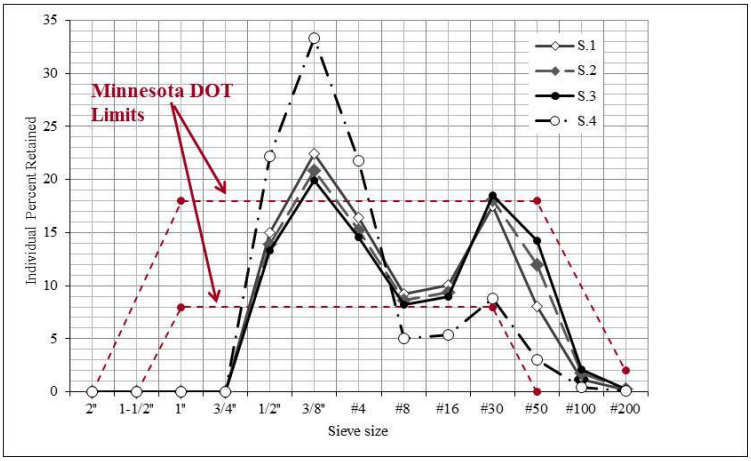

Fig.18 Comparison of the results with the limitation suggested by Minnesota DOT

Comparing the results with the limitation suggested by Minnesota DOT, it can be said that results of composition "S3" is placed better between the limit lines. According to his graph, except S4, all results are acceptable. Additionally Richardson, David N., (2005), has pointed out that the stone skeleton formulated with few voids (like composite S4) tended to be harsh. Thus the suitable aggregate composition to have the better fresh and dry concrete behavior seems to be composition S3. However the final selection will be due to the effects of the solid skeleton in the concrete mix.

5 FINDING THE OPTIMUM RATIO OF PASTE TO AGGREGATE SKELETON

Mix method used for the self-compacting concrete is significantly different from the typical method as well as its rating standards and testing since the design of method needs to consider the two opposite properties of flowability and segregation resistance

ability at the same time to assure the compacting capacity of the concrete (Choi et al. 2006). SCC has also the capacity to evolve the spaces between any obstacles. In addition segregation of the SCC components can be avoided controlling the viscosity and the cohesion of the mixture. In general, SCC has higher content of cement than conventional concrete, which requires extra cautions during its curing procedure to avoid crack formation, mainly in elements that have some restrictions to its deformation. (Barros Joaquim, et al. 2005).

At this step of the present work, the final SFRSCC compositions should result from the summation of the two distinct phases (the Agg. phase and the past phase), which its compositions are defined and optimized separately in the previous steps.

Testing different solid compositions (S1 to S4) is shown that using a lot of large aggregates, would give raise the concrete segregation. Thus the mixes made using compositions S4, S1, S2 and S3 respectively cased less segregation. But even using composition S3 which almost can be placed between the limitations introduced by Minnesota DOT could not be helpful to avoid the segregation problem. Using the same graph and the experiments achieved by testing the said Agg. skeletons leads to reduce the gap between the amount of large stones and fine sand, by increasing the amount of river sand (Agg. Composition S5 to S9). Thus by improving the property of the presented solid compositions the new series of composition is made. The effect of these Agg. compositions (which their sieve analysis is presented in Fig.19) on the workability of concrete is checked by performing the slump test on SCC made by these compositions. Between all the prepared concrete mixes the mix made using stone skeleton "S9" was helpful enough to increases viscosity in its fresh condition avoids the material segregation and stabilizes its quality. S9 composition includes 37% coarse aggregate, 51% river sand and 12% fine sand as shown in red color. Using the same solid composition, several SCC mix is made with different dosage of paste/aggregate skeleton ratio.

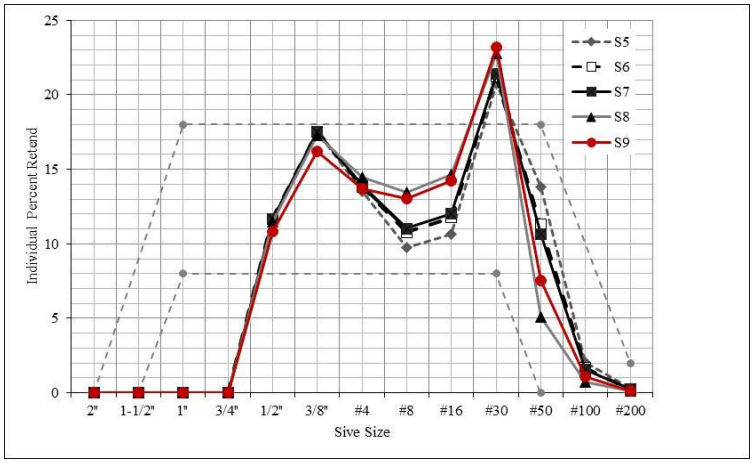

Fig.19 Individual percent retained

Thus, ratio of past to stone skeleton should be determined tacking in to account the workability and segregation resistance properties of SCC. In the present study it is observed that by increasing the percentage of past the distance between the solid particles and consequently the workability increase. The percentage of pest should be control such that after performing the slump test (to check to workability of the composition) the extra past should not be observed around the area of the spread concrete (Fig 20). To increase the workability it should be taken in to account that

increasing the w/c ratio is not a very good way. Increasing the water leads to disturb the structure of the optimized past. In addition, it makes the past watery, so that the past passes easily between the solid particles without helping the flowability, and leads to segregation (Fig.20).

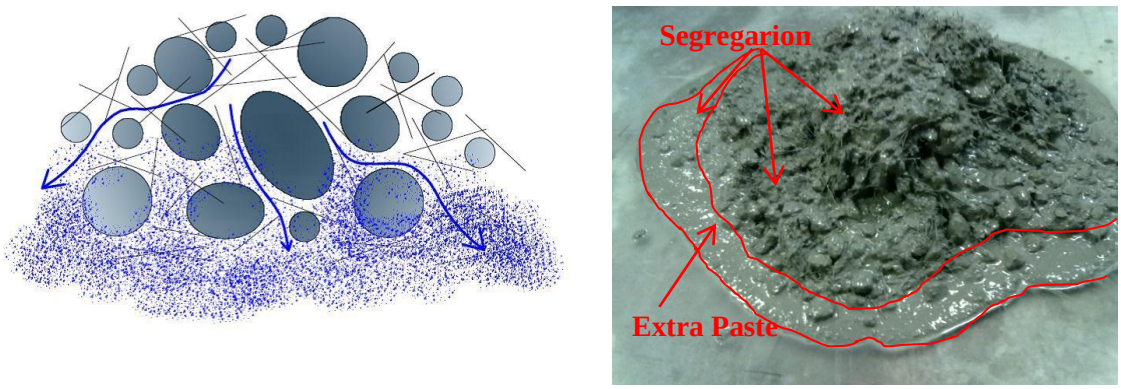

Fig.20 Segregation observed in SCC

When concrete compositions include steel fibers, flowability is lower, as steel fibers increase the resistance to flow (Johnson C. D., 2001). The slump flow test is used to assess the horizontal free flow of SCC in the absence of obstructions. It can also detect, by visualization, the occurrence of segregation (Barros Joaquim, et al. 2005).
In order to achieve the optimum content of paste on the final concrete mix, the percentage of the paste on the total concrete volume was varied in different mixes. The procedure of making the composition was as follow:

- The fine sand, river sand and crushed stone were discharged on the interior of the mixer, and were mixed with the amount of water needed for saturating them, for 30 seconds. The fine materials were added and mixed for 1 minute;
- 90% of the mixing water, with 10% of the amount of super plasticizer dissolved, was continuously added to the mix and uniformly distributed for 30 seconds, The rest of water and super plasticizer was gradually added to the composition and the mixing process continued for 1 minute more;
- After finding the homogenous composition, the steel fibers were added to the mix. The mixing process was stopped two minutes after. The total mixing time was 7 minutes.

Table-9 Concrete compositions executed with different paste percentages

Mix	Past Volume (%)	C Kg/m^3	FA Kg/m^3	LF Kg/m^3	W L/m^3	SP L/m^3	FS Kg/m^3	RS Kg/m^3	CS Kg/m^3	SF Kg/m^3
A	47	465	139	139	196	15.8	100	711	512	90
B	48	465	139	139	206.2	15.8	99	697	502	90
C	48.3	465	139	139	208.9	15.8	98	693	500	90
D	48.5	468	140	140	208.8	15.9	98	691	498	90
E	48.6	470	141	141	208.8	16	97	689	497	90

In a preliminary stage, for convenience, the flow behavior was only evaluated on the basis of visual inspection. As soon as the visually suitable SCC reached, the flowability, passing ability and compressive and tensile strength of the corresponding concrete was

evaluated. The total spread and flow time performance, accessed with the Abrams cone test. The compressive strength was evaluated from direct compression tests on cylinder samples, with a diameter of 150 mm and 300 mm high; and finally the tensile strength was tested using $150 \times 150 \times 600\ mm^3$ beam.
Table-9 shows the different ratios of past/stone skeleton. The best volume percentage of past has found around 48% during these tests (Fig.22 C). Using less past/stone skeleton ratio leads to the low flowability (Fig.22 A and B). The higher value leads to have the extra amount of past which may do nothing except increasing the cost of concrete and reducing the compressive strength. Comparing the fresh property of the concrete mixes which are shown in the following table, shows that mix C can be more acceptable.

Fig.22 Slump flow of SCC contains 47% (A), 48% (B) and 48.6% (C) past

6 MECHANICAL PROPERTY OF THE OPTIMIZED SCC

To increase the knowledge on the mechanical properties of the developed HPFRC, compressive strength as well as splitting and tensile strength of concrete is tested at the harden stage. The achieved results are briefly explained as follow:

6.1 Compressive Strength

Three cylinder specimens 300mm high with 150mm diameter made of the optimized SCC is used for performing the compressive test. The average compressive strength of the specimens is mentioned as Table-10.
The typical failure mode observed in the specimens tested under uniaxial compression is schematically depicted in Figure23 (a).
In general a vertical crack is occurred in the beginning of the softening phase by applying the compressive stress. This crack is continued by opening and sliding up to

the end of the test. Additionally the compressive struts separated by vertical cracks are observed on the concrete surface. This behavior leads to dissipation of energy due to the crack opening and sliding as shown in Fig.23 (b) (Cunha Vitor, 2010).
Since the fibers resist the crack opening occurs due to the friction of the concrete surface and aggregate interlock, the energy dissipation is higher in the case of FRSCC as compare to that of normal concrete.

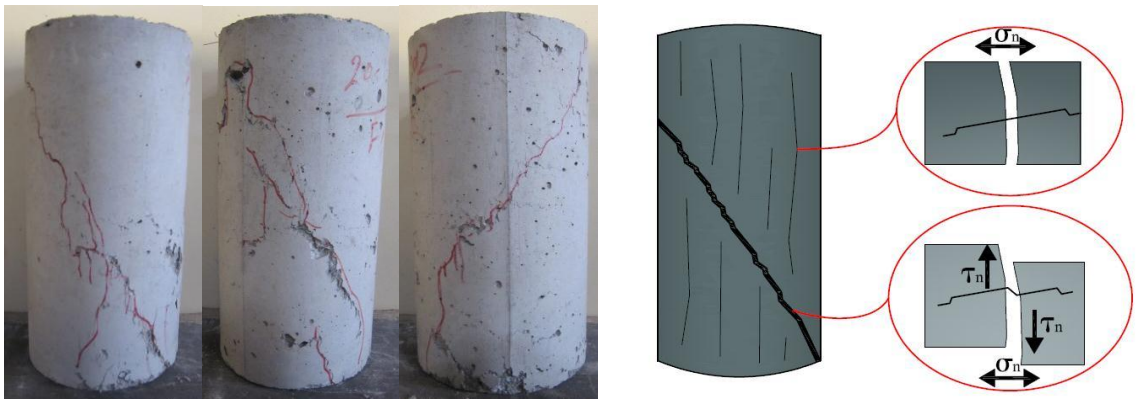

(a) (b)

Fig.23 Scheme of the failure modes observed in the compressive test (a) of the developed HPFRC (b) in general (Cunha Vitor, 2010)

Table-10 Compressive strength and Young's modulus of HPFRC

HPFRC Age *(day)*	f_{cm}[1] *(MPa)*	f_{ck} *(MPa)*	Young's modulus *(N/mm²)*	Concrete grade
3	44.27	36.27	27177	-
28	67	59	NA	60

[1] Mean value from two cylinder specimens;

In the case of the developed high strength concrete, the crack sliding occurs easier than that of normal strength concrete. The reason is that the fibers cannot resist the crack sliding as strong as fiber pullout in the compressive test. Thus when the highly confined concrete zones, provided by the machine steel plates, are displaced due to the applied load, the principal stresses in the contour of these zones are forming inclined micro-cracks that degenerate into a shear failure crack band.

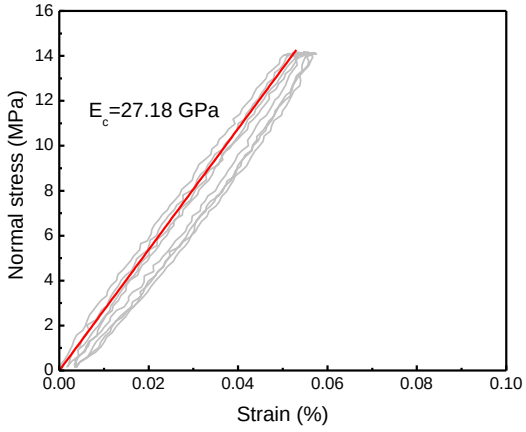

Fig.24 linear stress-strain relationship of 3days age HPFRC for determining the modulus of elasticity

6.2 Tensile Strength

According to RILEM TC 162-TDF (2002) recommendation, the tensile behavior of SFRSCC is obtained using the prismatic specimens of $150 \times 150\, mm^2$ cross section and 600mm length. The created notch which is located at the mid span of the beams on the surface perpendicular to the casting surface is 5mm thick and 25mm high. In order to ignore the crack branching occurs during loading the beams due to the high amount of fibers, two other beams are prepared including the deeper notch. The created notches are 6mm high.
The specimens were placed on roller supports, giving to the beam the free span of 500mm. The crack mouth opening displacement (CMOD) and the vertical displacement is measured using two LVDTs as shown in Fig. 24. The test is performed based on the displacement control with the constant rate of 0.2 mm/s.

Fig.24 Three-point bending test with the notch (left) 25mm and (right) 60mm high

Fig.25 (a) and (b) is depicted the load - defection and stress-CMOD relationship of the beams respectively. Since the beams are included the high content of fibers, the non-linear behavior is observed up to the peak load. Attaining the peak load, a plateau is observed up to a defection of nearby 1.5 mm. Reducing trend of the load is not very sharply in the post pick.
Crack branching is observed in the case of all the beams. Although the created notch is very deep in the beams included 6mm notch, the crack branching is observed due to the high volume percentage of the fibers (Fig.24). Table-11 includes the characteristic values of the post-peak parameters obtained from the three-point bending tests.

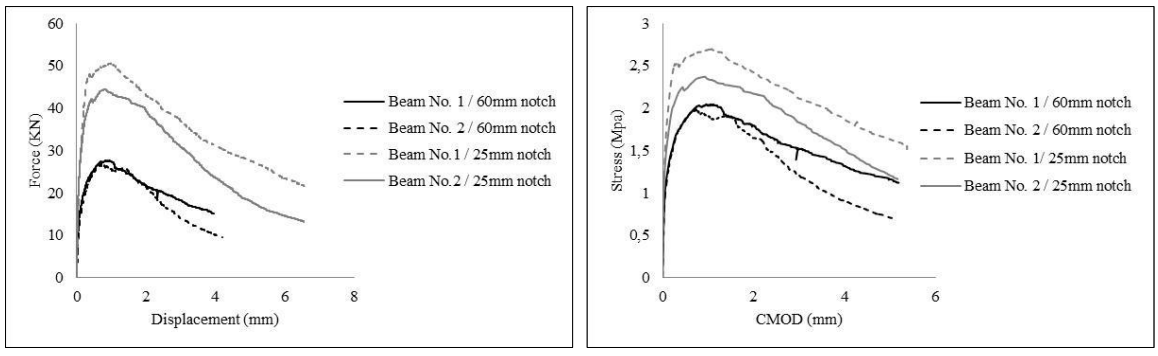

(a) (b)

Fig.25 (a) Load-deflection and (b) stress-CMOD relationship of the loaded beams

Since the crack branching is observed even after increasing the depth of the notch, some new specimens $150 \times 150 \times 600\, mm^3$ dimension, included 25mm notch are made. The created notch is located at three sides of the beam at the mid span as shown in Fig.26 a. The specimens are tested at the age of 3 days and the crack propagation is located along the notched ligament only (Fig.26 b). The achieved results are shown as Table-12 and Fig.27.

Table-11 Average and characteristic results of the three point bending tests of the 28days age HPFRC beam

Beam No.	Notched beam geometry			F_L	δ_L	F_{R1}	F_{R4}	f_{eq2}	f_{eq3}	$f_{R,1}$	$f_{R,4}$
	l *(mm)*	b *(mm)*	h_{sp} *(mm)*	*(KN)*	*(mm)*	*(KN)*	*(KN)*	*(MPa)*	*(MPa)*	*(MPa)*	*(MPa)*
B1	500	150	125	17.65	0.05	47.53	38.90	10.84	13.75	15.21	12.45
B2	500	150	125	20.3	0.05	41.42	30.83	9.48	12.19	13.25	9.87
B3	500	150	90	11.69	0.05	24.93	18.22	11.13	13.83	15.39	11.26
B4	500	150	90	9.74	0.05	24.51	14.03	10.80	13.27	15.13	8.66
Average				14.85	0.05	34.60	25.50	10.56	13.26	14.75	10.56

Table-12 Average and characteristic results of the three point bending tests of the 3days age HPFRC beam

Beam No.	Notched beam geometry			F_L	δ_L	F_{R1}	F_{R4}	f_{eq2}	f_{eq3}	$f_{R,1}$	$f_{R,4}$
	l *(mm)*	b *(mm)*	h_{sp} *(mm)*	*(KN)*	*(mm)*	*(KN)*	*(KN)*	*(MPa)*	*(MPa)*	*(MPa)*	*(MPa)*
B1	500	100	125	8.04	0.02	17.89	28.81	5.52	8.61	5.72	9.22
B2	500	100	125	9.86	0.04	16.88	22.04	4.42	6.63	5.40	7.05
Average				8.95	0.03	17.39	25.50	4.97	7.62	5.56	8.14

(a) (b)

Fig.26 (a) Notched beam configuration (b) location of the crack along the notched ligament

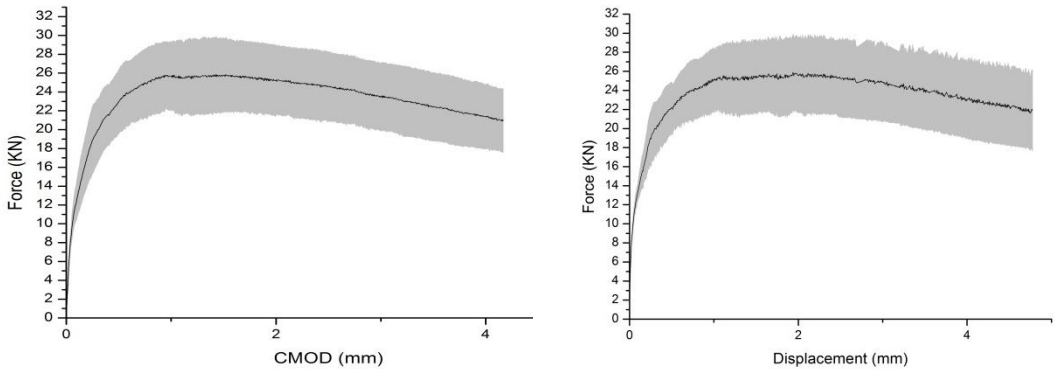

Fig.27 (left) stress-CMOD and (right) Load-deflection relationship of the loaded beams

6.3 Splitting Tensile Strength

The specimens used for the splitting test are obtained from the extremities of the tested bending specimens. Two $150 \times 150 \times 150\ mm^3$ cubic specimens are swan out from the prismatic bending specimens (Fig.26 a) according to BS 1981: Part 117 (1983). Two notches 5mm width and 15mm depth are created on the surface of the specimen which is helpful to localize the opening cracks.

Using this test, the splitting tensile behaviour of the HPFRC is identified (Fig.26 b). The splitting test responses has a similar behaviour to the one observed for the bending tests. Fig. 26 (c) depicts the experimental load versus crack opening mouth displacement relationship of the introduced specimens after 28days of casting.

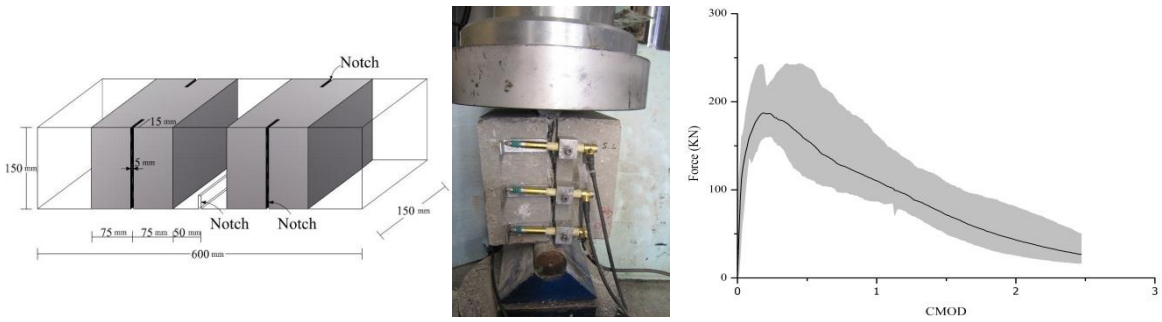

(a) (b) (c)

Fig.26 (a) Location and geometry of the specimen (b) test set-up and (c) load-CMOD relationship obtained using splitting tensile test

7 CONCLUSION

In the present study a HPFRC with the average compressive strength of 67MPa is developed using the special strategy. The introduced strategy is helpful to increase the workability of the concrete including the high amount of steel fiber whit out occurrence of segregation. It is helpful to increase the compactness of concrete as well as compressive and tensile strength.

During the development process of the HPFRC the rheological and mechanical properties of the concrete is evaluated. The shear behavior of the developed mix can be found in technical report No. 12-DEC/E-18 (Soltanzadeh et al. 2012).

Reference

1. Aïtcin, P.-C. (1998), "High-Performance Concrete," *E & FN SPON*, London.
2. Ahn, N., (2000), "An Experimental Study on the Guidelines for Using Higher Contents of Aggregate Microfines in Portland Cement Concrete," Ph.D. Dissertation, University of Texas at Austin.
3. Alexander, M.G., (1989), "Role of Aggregates in Hardened Concrete," Material Science of Concrete III, Skalny, J. and Mindess, S. eds., The American Ceramic Society, Inc. Westerville, Ohio, pp. 119-146.
4. ASTM C 305-91, (1991), "Standard Practice for Mechanical Mixing of Hydraulic Cement Pastes and Mortars of Plastic Consistency".
5. ASTM C 29/C 29M – 97, (1997), (Reapproved 2003) "Standard Test Method for Bulk Density ("Unit Weight") and Voids in Aggregate1".
6. ASTM C39 / C39M – 05, (2005), "Standard Test Method for Compressive Strength of Cylindrical Concrete Specimens".

7. ASTM C 939-02, (2002), "Standard Test Method for Flow of Grout for Preplaced-Aggregate Concrete (Flow Cone Method)," Annual book of ASTM standard, Vol., 04.02.
8. ASTM C-33, (1994), "Specification for Concrete Aggregates," West Conshohocken, Pa., ASTM. 04.02:8.
9. BS 1981: Part 117, (1983), "Testing concrete method for determination of tensile splitting strength".
1. British Standard Institute.
2. Chandra, S. Chapter five - Properties of concrete with mineral and chemical admixtures, 140–85. Spon Press (2002).
3. Choi Yun Wang, Kim Yong Jic, Shin Hwa Cheol, Moon Han Young, (2006), "An experimental research on the fluidity and mechanical properties of high-strength lightweight self-compacting concrete," Cement and Concrete Research 36, pp. 1595– 1602.
4. Cunha Vitor, (2010), "Steel Fibre Reinforced Self-Compacting Concrete," Doctoral Thesis, School of Engineering, Dept. of Civil Engineering, University of Minho, Guimarães, Portugal.
5. De Larrard, F. (1989), "Ultrafine Particles for the Making of Very High Strength Concretes," *Cement Concrete Research*, No. 2, pp. 161-171.
6. De Larrard, F., (1999), "Concrete Mixture Proportioning: A Scientific Approach," London.
7. Felekoğlu Burak, Türkel Selc-uk, Baradan Bülent, (2007), "Effect of water/cement ratio on the fresh and hardened properties of self-compacting concrete," Building and Environment 42, pp 1795–1802.
8. Ferrara, L., Park Y., Shah, S. P., (2007), "A method for mix-design of fiber-reinforced self-compacting concrete," *Journal of Cement and Concrete Research*, 37, pp 957–97.
9. Gomes, P. C. C., (2002), "OPTIMIZATION AND CHARACTERIZATION OF HIGH-STRENGTH SELF-COMPACTING CONCRETE," Doctoral Thesis, Universitat Politècnica de Catalunya Escola Tècnica Superior d'enginyers de Camins, Canals I Ports de Barcelona.
10. Grünewald S., (2004), "Performance-based design of self-compacting fibre reinforced concrete," PhD Thesis, Delft University of Technology.
11. Jansson Anette, (2008), "Fibres in reinforced concrete structures analysis, experiments and design," Doctoral Thesis, Department of Civil and Environmental Engineering, Division of Structural Engineering, CHALMERS UNIVERSITY OF TECHNOLOGY, Göteborg, Sweden.
12. Johnston, C. D., (2001), "Fiber-Reinforced Cements and Concretes," Gordon and Breach Science Publishers.
13. Legg, F.E. Jr., (1998), Aggregates, Chapter 2, Concrete Construction Handbook, ed. Dobrowolski, J. McGraw-Hill, 4th ed.
14. Mehta, P. K. and Monteiro, P. J., (1993), "Concrete: Structure, Properties, and Materials," Prentice-Hall, Englewood Cliffs, N.J., 2nd ed,.
15. Nakamura, S., van Mier, J.G.M., and Masuda, Y., (2004), "Self compactability of hybrid fiber concrete containing PVA fibers", in M. di Prisco et al. (eds.) BEFIB 2004, Proc. 6th Int. RILEM Symp., Varenna, Italy, 20-22 Sept., Rilem Pubs.,pp. 527-538.
16. Noor MA, Uomoto T. Three-dimensional discrete element simulation of rheology tests of self-compacting concrete. First international RILEM

symposium on self-compacting concrete, Rilem Publications s.a.r.l., 1999. p. 35‑46.
17. Ozyurt N, Mason TO, Shah SP, (2007), "Correlation of fiber dispersion, rheology and mechanical performance of FRCs," *Cement and Concrete Composites*, 29:70-79.
18. Gomes Paulo César Correia, (2002), "optimization and characterization of high-strength self-compacting concrete," Doctoral Thesis, Universitat Politècnica de Catalunya Escola Tècnica Superior d'enginyers de Camins, Canals I Ports de Barcelona.
19. Okamura, H. and Ouchi, M., (1999), "Self-Compacting Concrete. Development, Present use and Future", Proc. 1st International RILEM Symposium on Self-Compacting Concrete (Stockholm, Sweden), A. Skarendhal and O.Pstersson (editors), RILEM Publications S.A.R.L.
20. Pereira, Eduardo Nuno Borges, (2006), "Steel fiber reinforced self-compacting concrete: from material to mechanical behavior," Doctoral Thesis, School of Engineering, Dept. of Civil Engineering, University of Minho, Guimarães, Portugal.
21. Quiroga, Pedro Nel and Fowler, David W., (2004), "The effects of aggregates characteristics on the performance of Portland cement concrete," Research Report ICAR – 104-1F, International Center for Aggregates Research, The University of Texas at Austin, University Station C1755 Austin, TX 78712-0277.
22. Ravikumar M. S., Selvamony C., Kannan S. U., and Gnanappa Basil S., (2009), "Behavior of self-compacted self-curing kiln ash concrete with various admixtures," *ARPN Journal of Engineering and Applied Sciences*, VOL. 4, NO. 8, pp. 25-30.
23. Richardson, David N., (2005), "Aggregate gradation optimization- literature search," Technical Report, RDT 05-001, University of Missouri- Rolla.
24. Shilstone, J. M. Sr., (1994), "Changes in Concrete Aggregate Standards," The Construction Specifier, p. 119.
25. Shilstone, J. M., (1999), "The Aggregate: The Most Important Value-Adding Component in Concrete," Proceedings, Seventh Annual International Center for Aggregates Research Symposium, Austin, Texas.
26. Shilstone, J. M. Sr., (1990), "Concrete Mixture Optimization," Concrete International: Design and Construction, Vol. 12, No. 6, pp. 33-39.
27. Shilstone, J.M. and J.M. Shilstone Jr., (1987), "Practical concrete mixture proportioning technology, reference manual," Shilstone Software Co., quoted in: Richardson, David N., (2005), "Aggregate gradation optimization- literature search," Technical Report, RDT 05-001, University of Missouri- Rolla.
28. Soltanzadeh F., (2010), "Properties of HSC at elevated temperatures," Master Thesis, Department of Civil Engineering, Zakir Husain College of Engineering and Technology, Aligarh Muslim University, Aligarh, India.
29. Soltanzadeh F., Barros J. A. O. and Santos R. F. C., "Study of the fracture behaviour of fiber reinforced concrete under direct shear loading," Technical Report No. 12-DEC/E-18, University of Minho, May 2012.
30. UASF (1997). United States Air Force Guide Specification, Militry Airfield Construction, Rigid Airfield Pavement Surface. U. S. A. Force: 1-33. Quoted in: "Richardson, David N., (2005), "Aggregate gradation optimization- literature search," Technical Report, RDT 05-001, University of Missouri- Rolla".

31. Washa, G.W., (1998), Workability, Chapter 5, Concrete Construction Handbook, ed. Dobrowolski, J. McGraw-Hill, 1998, 4th ed., New York.
32. Grünewald Steffen, Walraven Joost C., (2009), "Transporting fibres as reinforcement in self-compacting concrete," *HERON*, Vol. 54, No. 2/3, pp 101-126.
33. Barros Joaquim, Pereira Eduardo, Cunha Vítor, Ribeiro Alberto, Santos Simão, Queirós Paulo, (2005), "Paberfia – Lightweight Sandwhich Panels of Steel Fiber Reinforced Self Compacting Concrete," Report, PRÉGAIA, S.A. / CiviTEST, Lda. / University of Minho.
34. RILEM TC 162-TDF (2002b). Test and design methods for steel fiber reinforced concrete-bending test (final recommendation), *Journal of Materials and Structures*, 35(253), 579-582.